School of Chinese Pharmacy[1]; Department of Pathology[2], Beijing University of Chinese Medicine, Beijing, China

A new ligustrazine derivative - pharmacokinetic evaluation and antitumor activity by suppression of NF-κB/p65 and COX-2 expression in S180 mice

Penglong Wang[1], Yuzhong Zhang[2], Kuo Xu[1], Qiang Li[1], Honggui Zhang[1], Jing Guo[1], Dandan Pang[2], Yatao Cheng[1], Haimin Lei[1]

Received January 14, 2013, accepted February 11, 2013

Prof. Haimin Lei, School of Chinese Pharmacy, Beijing University of Chinese Medicine, 6 Wangjing Mid Ring South Road, Beijing 100102, China
hm_lei@126.com

Pharmazie 68: 782–789 (2013) *doi: 10.1691/ph.2013.3515*

A new anticancer ligustrazine derivative, 3β-hydroxyolea-12-en-28-oic acid-3,5,6-trimethylpyrazin-2-methyl ester (T-OA, $C_{38}H_{58}O_3N_2$), was previously reported. It was synthesized via conjugating the effective anti-tumor ingredients of a classic traditional Chinese medicine (TCM) formulation. In the present study, anticancer efficacy of T-OA was evaluated *in vivo* using a murine sarcoma S180 model. Reduction of the tumor weight and tumor HE staining regions demonstrated that T-OA had promising inhibition effects and a 50% inhibitory rate in S180 mice. Combining the immunohistochemistry, we found T-OA exerted its antitumor activity by preventing the expression of nuclear transcription factor NF-κB/p65 and COX-2 in S180 mice. The acute toxic test showed that LD_{50} value of T-OA exceeded 6.0 g/kg via gavage in mice. In addition, a simple and rapid HPLC–UV method was developed and validated to study the pharmacokinetic characteristics of the compound. After single-dose oral administration, time to reach peak concentration of T-OA (3.97 μg/mL) was 8.33 h; the elimination half-life and area under the concentration–time curve from $t = 0$ to the last time of T-OA was 4.50 h and 48.01 μg·h/mL, respectively.

1. Introduction

The attempt to apply 'combination principle' to discover lead compounds from traditional Chinese medicine (TCM) formulations has already drawn considerable attention (Zhang et al. 2009a, b; Hao et al. 2010; Wang et al. 2013, 2012). In our earlier study of this field, a series of ligustrazine derivatives were synthesized via conjugating the anti-tumor bioactive compounds from one classic TCM prescription, Shiquandabu Wan, which is widely used to treat cancer in Chinese communities (Wang et al. 2012; Ni et al. 2005; Yin et al. 2011; Zhang et al. 2007). The anti-tumor evaluation showed that 3β-hydroxyolea-12-en-28-oic acid-3,5,6-trimethylpyrazin-2-methyl ester (T-OA, $C_{38}H_{58}O_3N_2$), conjugated by one tetramethylpyrazine (TMP) and one oleanolic acid (OA) via ester bond (Fig. 1), had promising anti-cancer activities on Bel7402 and HCT-8 tumor cells with $IC_{50} = 7.611$ μg/mL and 9.273 μg/mL, respectively.

In this investigation, we screened the T-OA antitumor effect in a murine sarcoma S180 model, which could directly evaluate the agents' tumor inhibition and toxicity; moreover, this model was also used to elucidate the antitumor mechanisms (Liao et al. 2012; Wu et al. 2010; Chen et al. 2012; Jiang et al. 2011). Both TMP and OA, the starting materials of T-OA, have earlier been documented as inhibitors of nuclear factor-κB (NF-κB) (Li et al. 2009; Suh et al. 2007). NF-κB, a transcriptional factor, plays a central role in regulating inflammatory and immunological processes; it influences the expression of cyclooxygenase-2 (COX-2) and is critically involved in tumor progression due to its transcriptional regulation of invasion-related factors (Aggarwal 2004; Orlowski and Baldwin 2002; Suauki et al. 2006; Plummer et al. 1999). In addition, numerous studies have demonstrated

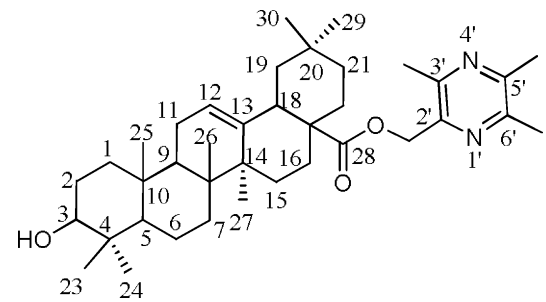

Fig. 1: Structure of T-OA.

that COX-2 expression increased during progression from normal to cancerous state; COX-2 stimulates angiogenesis and is associated with tumor growth, invasion, and metastasis (Tang et al. 2005; Mazhar et al.2005; Sarkar et al. 2007; Zhong et al. 2012; Cathcart et al. 2012). For these, both NF-κB and COX-2 have been identified as important mediators of malignancy and therefore served as important targets for antitumor drug development and discovery (Nagendraprabhu and Sudhandiran 2011; Olivera et al. 2012; Sivaramakrishnan and Niranjali 2009; Santhi et al. 2006; Breinig et al. 2007). In the light of recent knowledge about the importance of regulation of NF-κB and COX-2 activities, immunohistochemistry analysis was employed to investigate T-OA's effects on the expression of NF-κB/p65 and COX-2 in S180 mice.

Moreover, acute toxic test, as a part of safety evaluation of T-OA, was carried out to investigate the potential toxicity after orally dosing maximum T-OA in Kunming mice. In addition, an important part of the preclinical development of a new anticancer

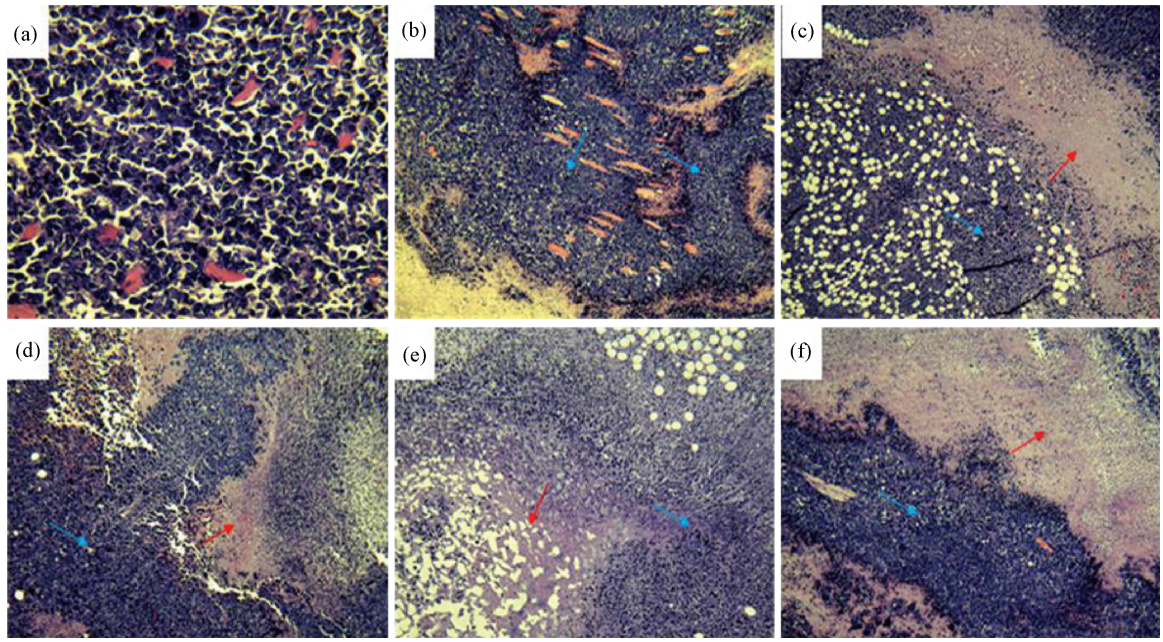

Fig. 2: Anti-tumor effect of T-OA by HE staining. (a) Model group (×400), the tumor cell nucleus were dyed in brown stains in (a). (b) Model group (×100). (c) CTX group (×100). (d) Low dose of T-OA group (×100). (e) Middle dose of T-OA group (×100). (f) High dose of T-OA group (×100); the blue arrowhead was tumor tissue; the red arrowheads were the tumor necrotic regions after drugs administration.

therapeutic is to investigate the pharmacokinetic characteristics (Lee et al. 2012; Qiu et al. 2012). Thus, a reliable HPLC-UV method was developed to separate and quantify T-OA in rat plasma. Then we applied this method to study T-OA's pharmacokinetics after oral administration to Sprague–Dawley (SD) rats.

2. Investigations, results and discussion

2.1. T-OA's antitumor activity in vivo

Treatment with the three T-OA doses resulted in marked suppression of tumor weight in a dose-dependent manner (Table 1). Compared with the model group, the inhibitory rates of T-OA were 33.98%, 37.23% and 50.00% at the doses of 75, 150, and 300 mg/kg, respectively; while cyclophosphamide (CTX) caused 73.40% inhibition. The growth of implanted sarcoma S180 tumor in mice could be significantly inhibited by the high T-OA dosage group ($p < 0.05$). Moreover, HE staining also directly showed that both high T-OA dosage (Fig. 2f) and CTX groups' (Fig. 2c) tumor necrotic regions significantly increased over the model group (Fig. 2b) ($p < 0.05$). The tumor cells of the model group exhibited a high mitotic index, obvious atypia (Fig. 2a and b), whereas tumor cells proliferation of the treated groups were blockaded in some way. Meanwhile, we could clearly observe that the necrosis regions of the tumor nests significantly increased with increasing concentration of T-OA (Fig. 2 and 3).

Furthermore, the liver indices, which were similar in the normal and T-OA treated groups ($p > 0.05$), indicated that T-OA did not cause serious toxic effects on the liver system (Xu et al. 2012). Spleen is one of the main immune organs; it is responsible for initiating immune reactions in the body. Thus the spleen index directly reflects the status of the immune system (Cesta 2006). Spleen indices of T-OA treated groups were higher than both the normal and CTX groups' (Table 1). Increases in spleen index suggested that T-OA could regulate the immune system of S180 mice (Liao et al. 2012).

During the ten days' chemotherapy with CTX after tumor implanted, the activities of mice in CTX group were becoming slow, listless and emaciated, while there were no signs of general clinical symptoms of toxicity or abnormal behavior and no mortality in T-OA groups. These results indicated that there was no significant toxicity with the treatment of T-OA, and the following acute toxic test also displayed that T-OA did not show toxicity in mice.

2.2. T-OA inhibit the expression of nuclear transcription factor NF-κB/p65 and COX-2 in murine sarcoma S180 model

NF-κB is an ubiquitous transcription factor in various cells involved in inflammatory reactions, and exerts its effects by expressing cytokines, chemokines, cell adhesion molecules and growth factors (Lee and Burckart 1998). S180 cells were not implanted in to normal group mice, so liver tissue of normal mice was set as the control test. In immunohistochemistry analysis, the normal liver tissue showed weak expression of NF-κB/p65 (Fig. 4a). Tumor tissues of the model group displayed an increased expression of NF-κB/p65 that was evident

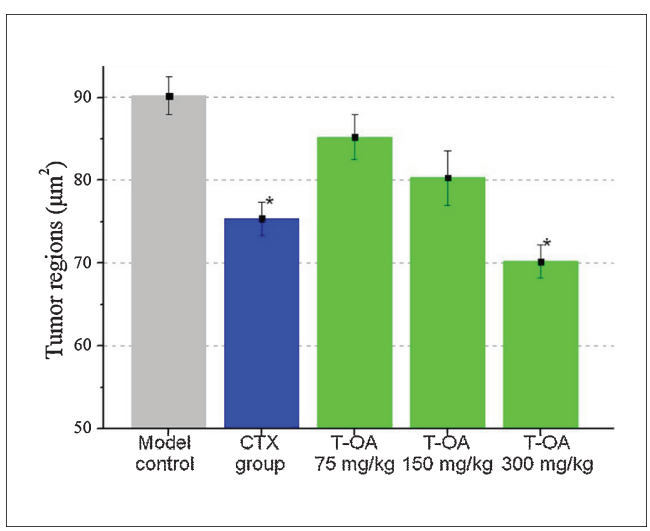

Fig. 3: Tumor regions with HE staining of model and treatment groups of S180 mice (n = 8).

Table 1: Effects of T-OA in S180 mice (mean ± S.D.)

Group	Dose (mg/kg)	Mice number start/end	Weight gain (g)	Tumor weight (g)	Inhibitory rate (%)	Liver index (100*g/g)	Spleen index (mg/g)
Normal group	——	10 / 10	7.23 ± 2.16	——	——	5.01 ± 0.46	4.10 ± 0.77
Model group	——	10 / 10	$9.57 \pm 2.15^{\#\#}$	0.94 ± 0.41	——	5.28 ± 0.48	4.33 ± 0.84
CTX	20	10 / 10	6.90 ± 2.04	$0.25 \pm 0.16^{**}$	73.40%	5.19 ± 0.33	3.93 ± 1.11
T-OA	75	10 / 10	$10.15 \pm 2.81^{\#\#}$	0.63 ± 0.30	33.98%	5.43 ± 0.59	4.36 ± 1.13
T-OA	150	10 / 10	7.54 ± 3.56	0.59 ± 0.28	37.23%	5.39 ± 0.46	$5.68 \pm 1.77^{\#}$
T-OA	300	10 / 10	7.72 ± 3.68	$0.47 \pm 0.23^{*}$	50.00%	5.45 ± 0.72	4.82 ± 2.23

$^{\#}$compared with normal group: $^{\#}$ $p < 0.05$, $^{\#\#}$ $p < 0.01$; * compared with model group: $^{*}p < 0.05$, $^{**}p < 0.01$.

from increased brown staining (Fig. 4b). However, S180 mice treated by CTX and T-OA (low, middle and high dose) exhibited a decrease in NF-κB/p65 expression compared with model group (Fig. 4c, 4d, 4e and 4f, respectively), and T-OA groups revealed in a dose-dependent manner expression of NF-κB/p65. The high dose of T-OA group's NF-κB/p65 expression greatly decreased and its inhibition effect was similar to that of the CTX group's, whose inhibition effect on NF-κB had been proved earlier (Mammon et al. 2006). This finding suggested that T-OA administration could prevent NF-κB/p65 activation, exert its antitumor effect possibly through disrupting NF-κB signaling in S180 tumors thus leading to cancer cells proliferation blockade. The immunohistochemical results of COX-2 were represented in Fig. 5. The results were similar to the immunohistochemical analysis of NF-κB. As COX-2 is expressed weakly in normal tissues, the liver tissue of normal group showed only negligible expression of COX-2 (Fig. 5a). However, the model group showed an increased brown stained expression of COX-2 in tumor tissue (Fig. 5b). In addition, T-OA (Fig. 5d, 5e and 5f, respectively) treated mice displayed a decreased expression of COX-2 compared with the model group (Fig. 5b) in a dose-dependent manner. The results were accordant with previous studies that some antitumor agents suppressed COX-2 expression via inhibition of NF-κB activity (Plummer et al. 1999; Yoon et al. 2005; Kang et al. 2011).

2.3. Acute toxicity test in vivo

Acute toxicity test is an important part of preclinical development of a new oral anticancer therapeutic. The relative body weight loss was used here as a measure of toxicity (Wu et al. 2010). The mice were randomly grouped on the basis of their body weight. At the beginning of administration, the weight showed no significant difference between the groups ($P > 0.05$). After oral administration of the maximum tolerated dose (6 g/kg/day), there was no mortality in each group and no signs of general clinical symptoms of toxicity or abnormal behavior appeared during two weeks. At the end of the experiment, there were no significant differences in body weights between treatment and control groups (Fig. 6).

2.4. Pharmacokinetic study

Administration of 300 mg/kg T-OA, led to a significant growth inhibition to the implanted S180 tumor at the end of treatment; but the dosage was higher than that of common antitumor agents and it was necessary for the further pharmacokinetic properties study to indicate an extrapolated bioavailability. To make an accurate and continuous monitoring of blood concentration, SD rats were chosen for the pharmacokinetics evaluation.

2.4.1. Method validation

2.4.1.1. Specificity

Typical chromatograms of T-OA in rat plasma are presented in Fig. 7. With the chromatographic conditions described in the Experimental part, satisfactory peak separation and resolution were achieved, and no endogenous substances or metabolites significantly interfered with the determination of T-OA. (3, 18, 20)-3-hydroxy-11-oxoolean-12-en-29-oicacid-

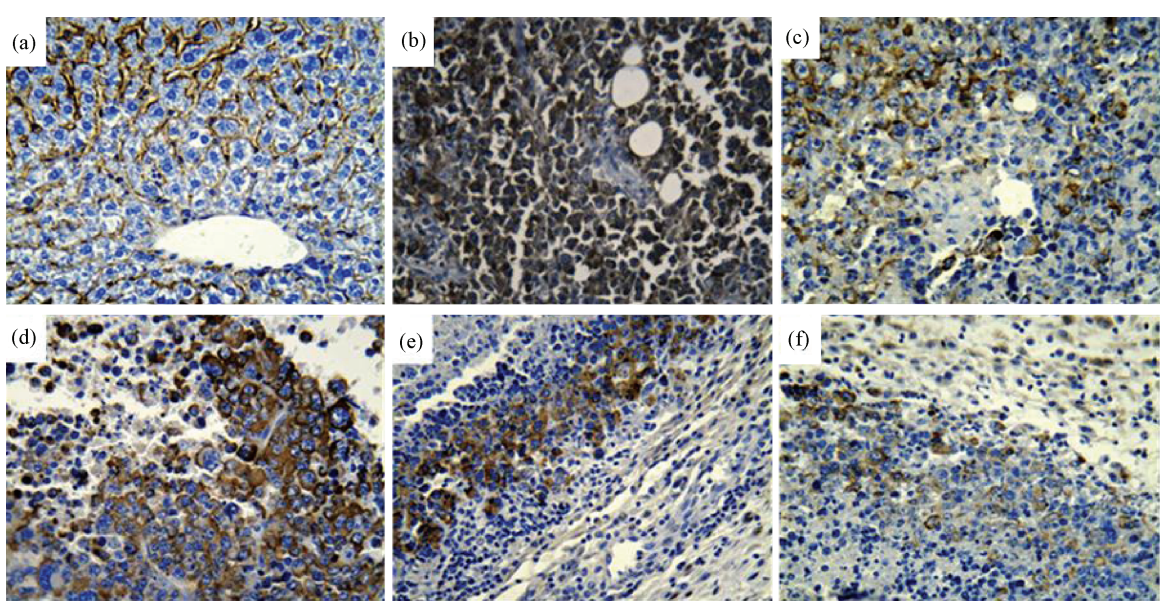

Fig. 4: Immunohistochemical analysis of NF-κB in control and experimental groups of mice. (a) Normal group (×100). (b) Model group (×100). (c) CTX group (×100). (d) Low dose of T-OA (×100). (e) Middle dose of T-OA (×100). (f) High dose of T-OA (×100).

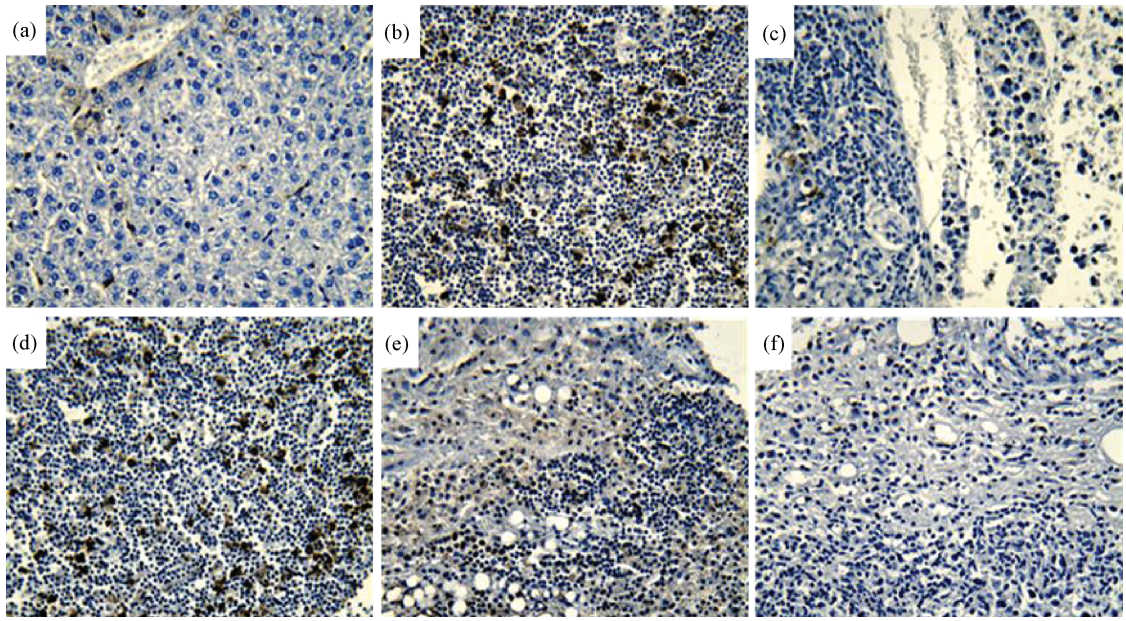

Fig. 5: Immunohistochemical analysis of COX-2 in control and treated groups of mice. (a) Normal group (×100). (b) Model group (×100). (c) CTX group (×100). (d) Low dose of T-OA (×100). (e) Middle dose of T-OA (×100). (f) High dose of T-OA (×100).

3,5,6-trimethylpyrazin-2-methyl ester, which had been reported in our previous study, was selected as internal standard (IS) because of its similar chemical structure, chromatographic behavior, efficient extraction (Fig. 7a) (Wang et al. 2012). The retention time for IS and T-OA was approximately at 7.6 and 10.6 min, respectively.

2.4.1.2. Calibration curve and linearity

The calibration curve was of good linearity within a range of 0.2050 – 8.2000 μg/mL in rat plasma, and the linear regression equation was Y = 0.5507 X – 0.0327 with a linear correlation coefficient (r) of 0.9995. X referred to ratio of T-OA peak area over the IS area; and Y was the concentration of T-OA in rat plasma.

2.4.1.3. Precision, accuracy, limit of detection, and quantitation

The intra- and inter-day precision and accuracy are summarized in Table 2. The intra- and inter-day precision was expressed as RSD, which ranged from 1.12 to 2.46% and 0.97 to 2.68%, respectively. The limit of detection was 0.1010 μg/mL and the limit of quantitation was 0.2050 μg/mL. The results indicated that the present method was reliable and reproducible for quantitative T-OA in biosamples.

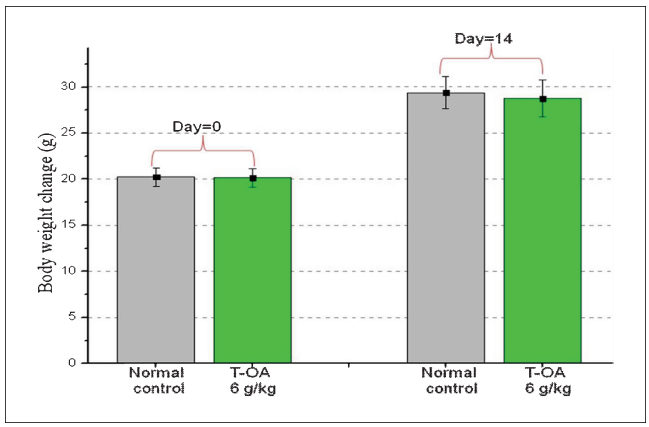

Fig. 6: Body weights change of each group at the first day (day 0) and the last day (day 14) after oral administration maximum tolerated dose (6 g/kg/day). *P < 0.05 compared with control group. All data were expressed as mean ± S.D. (n = 20).

2.4.1.4. Extraction recovery and stability

The relative extraction recovery and absolute extraction recovery of T-OA in rat plasma are summarized in Table 3. The mean relative recoveries of T-OA in plasma at three different concentrations (0.8250, 2.5625 and 6.5600 μg/mL) were 91.52, 103.95, 92.48%; and the mean absolute recoveries were 88.39, 90.27 and 86.51%, respectively. The recovery of IS was above 90%.

Freezing and thawing cycles did not significantly change the concentrations of T-OA. The mean amount of T-OA in plasma samples was found to be 98.90% of the initial value after three freezing–thawing cycles. The spiked plasma samples were found stable at room temperature for 24 h. After storing at room temperature for 24 h, T-OA's concentration in the reconstituted methanol solutions ranged from 99.42 to 100.51% of the initial concentration. Thus, these data indicated T-OA was stable in plasma samples during measurement; T-OA's biosample preparation procedure was satisfying and could achieve the believable results for its pharmacokinetic study.

2.4.2. Pharmacokinetic study and data analysis

The method developed in this study was selective for T-OA analyzed and no endogenous interference was observed on chromatograms. The mean plasma concentration-time profile of T-OA after oral administration (300 mg/kg) is shown in Fig. 8, with pharmacokinetic parameters summarized in Table 4. T-OA behaved according to the non-compartment model after single-dose oral administration in six rats. It was absorbed at a slow rate and reached the maximum plasma concentration (C_{max} value 3.97 μg/mL) within 8.33 h. The plasma concentration of T-OA declined with an elimination half-life of 4.50 h. The area under concentration–time curve from $t = 0$ to last time (AUC) (μg·h/mL) was 48.01 ± 11.21 for T-OA.

The pharmacokinetic study indicates that the extrapolated bioavailability of T-OA was less than 10%. The poor pharmacokinetic performance may be due to poor water-solubility that results from T-OA's relatively lipophilic structure. To raise T-OA's bioavailability, several pharmaceutical preparations are in progress. For example, the solid dispersion method as an

Table 2: Intra- and inter-day precision and accuracy of T-OA in rat plasma (mean ± SD, n=5)

	Intra-day			Inter-day		
Concentration added (μg/mL)	Concentration observed (μg/mL)	Accuracy (%)	Precision (RSD %)	Concentration observed (μg/mL)	Accuracy (%)	Precision (RSD %)
0.8250	0.8330 ± 0.0205	100.97 ± 2.48	2.46	0.7490 ± 0.0106	90.79 ± 1.28	1.41
2.5625	2.6540 ± 0.0318	103.57 ± 1.24	1.12	2.4934 ± 0.0241	97.30 ± 0.94	0.97
6.5600	5.9963 ± 0.0679	91.41 ± 1.04	1.13	6.2674 ± 0.1683	95.54 ± 2.57	2.68

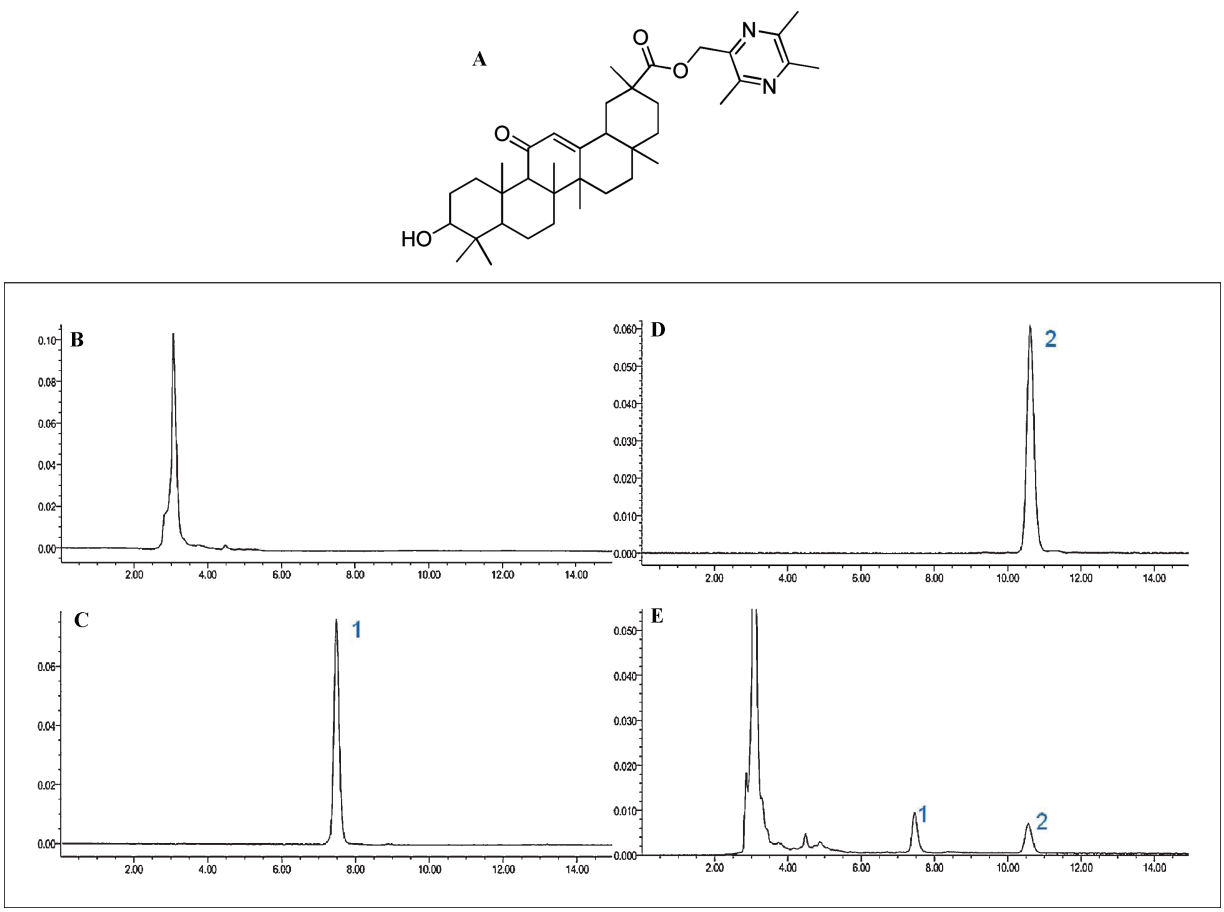

Fig. 7: Representative HPLC chromatograms of the analytes. (a) Structure of internal standard (IS); (b) Blank rat plasma; (c) HPLC chromatogram of IS; (d) HPLC chromatogram of T-OA; (e) Plasma sample collected at 4 h after administration of T-OA (300 mg/kg) added with IS; *1* IS; *2* T-OA.

approach for bioavailability enhancement of poorly water-soluble drug (Chiou and Riegelman 1971; Sinha et al. 2010; Leuner and Dressman 2000; Liu and Wang 2007; He et al. 2011), containing the fusion method and the solvent evaporation method, has been prepared to increase the water-soluble of T-OA. In addition, to enhance the permeability and intestinal absorption of T-OA *in vivo*, an oil-in-water micro emulsion form (diameter about 80 nm) of T-OA have been prepared successfully; a single-dose (300 mg/kg) oral pharmacokinetic study of this micro emulsion showed that peak plasma concentrations of T-OA could reach 12.95 μg/mL.

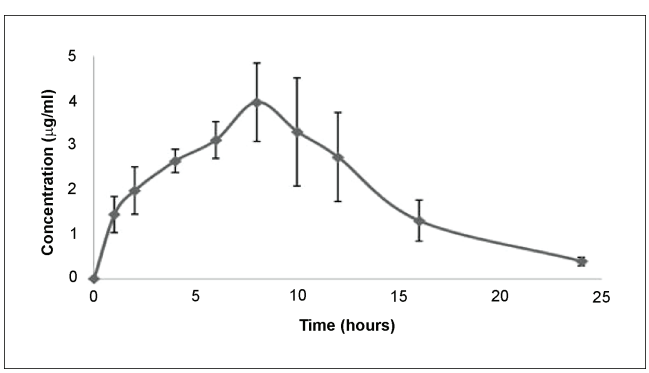

Fig. 8: Plasma concentration–time profiles of T-OA after oral administration (mean ± SD, n = 6).

2.5. Conclusions

In summary, our present study indicated that T-OA is a potent oral antitumor therapeutic with low toxicity. The antitumor mechanism tests suggested that T-OA exerts its antitumor activity by preventing the expression of NF-κB/p65 and COX-2 in S180 mice. Furthermore, we developed a simple and reliable HPLC method to quantify T-OA in rat plasma. The analytical method was successfully applied to identify the pharmacokinetic profile of T-OA in rats. It was found that T-OA had a longer elimination half-life than its parent compounds TMP and OA (Jeong et al. 2007; Xiao et al. 2007). Though the oral pharmacokinetic study produced a limited exposure, it indicated that T-OA could exert antitumor efficacy at a low blood concentration. Moreover, we found T-OA's oral bioavailability could be improved significantly through preparing the oil-in-water micro

Table 3: Extraction recovery of T-OA in rat plasma (mean ± SD, n = 5)

Concentration added (μg/mL)	Relative recovery		Absolute recovery	
	C_{obs} / C_{the}%	RSD%	A_{obs} / A_{the}%	RSD%
0.8250	91.52 ± 2.96	3.23	88.39 ± 2.41	2.73
2.5625	103.95 ± 1.91	1.84	90.27 ± 4.40	4.88
6.5600	92.48 ± 2.31	2.50	86.51 ± 3.77	4.36

Table 4: Main pharmacokinetic parameters of T-OA in rats

Parameters	Units	Mean ± SD
AUC_{last}	μg·h/mL	48.01 ± 11.21
CL	mL/h/kg	6194.82 ± 1422.85
V_z	mL/kg	40757.87 ± 13803.29
$t_{1/2}$	h	4.50 ± 0.82
C_{max}	μg/mL	3.97 ± 0.97
T_{max}	h	8.33 ± 0.82
MRT	h	9.43 ± 0.50

emulsion form; this part of work will be displayed in the near future. Based on the studies of pharmacology and pharmacokinetic evaluations, T-OA represented a valuable candidate for anticancer drug discovery and development.

3. Experimental

3.1. General

Murine sarcoma S180 cells provided by 302 military hospital of China were maintained in RPMI-1640 medium, supplemented with 10% fetal bovine serum (Hyclone, Aurora, Canada), 100 IU/ml Penicillin-Streptomycin (Hyclone), and Non-Essential Amino Acids (Sigma), at 37 °C under humidified air with 5% CO_2. Female/male Kunming mice and male SD rats (Beijing Vital River Laboratory Animal Technology Company Limited, China) were kept under standard laboratory conditions (tap water, constant room temperature 22 °C). Principles of laboratory animal care were followed and all experiments were carried out in accordance with the "Regulation for the Administration of Affairs Concerning Experimental Animals" (State Council of China, 1988).

Both T-OA and IS were synthesized in our laboratory as reported previously (Wang et al. 2012). The purity of T-OA and IS was > 99% by HPLC analysis. HPLC-grade methanol and acetonitrile were purchased from Xinkeao Scientific & Technology Co. Ltd (Beijing, China). Other chemicals and reagents were analytical grade and commercially available.

The LC system consisted of a Waters 2695 HPLC system (Waters Corporation, USA) and with column temperature set at 30 °C, using diode-array detection (Shimadzu SPD-M10A). The column used during pharmacokinetic assay was a reversed-phase Agilent TC-C18 analytical column (4.6 mm × 250 mm, 5 μm particle size) and was eluted at a flow rate of 1 mL/min solvent consisted of 95% MeOH and 5% aqueous solution. Detection wavelength was 278 nm. The injection volume was 10 μL.

3.2. Evaluation of anti-tumor effect in S180 mice

S180 cells were harvested and washed three times with RPMI-1640 medium. The cells were pelleted by brief centrifugation at 800 r/min for 10 min. The supernatant was aspirated, and the cells were resuspended in normal saline at a density of 2×10^7 cells/mL. Male Kunming mice were subcutaneously implanted with 2×10^6 cells/mouse on the left flank (day 0). Twenty-four hours after inoculation, 50 tumor bearing mice were randomly divided into model group, CTX group, high T-OA dose group, medium T-OA dose group, and low T-OA dose group (n = 10), respectively. Another 10 mice without any treatment were set as normal group.

T-OA (suspended in bean oil) was continuously administrated via gavage, once daily for 10 days. S180 mice in the high, medium and low T-OA dose groups received intragastric T-OA of 300, 150 and 75 mg/day per kg of body weight, respectively; the CTX group received CTX (20 mg/kg), model and normal groups were oral treated with bean oil, respectively.

Twenty-four hours after the last administration, the mice were sacrificed and the solid tumors, livers and spleens were excised and weighed. The inhibition rate (IR) of tumor growth was calculated by the following formula: IR (%) = [(A – B)/A]/100, where A is the average tumor weight of the model group, and B is that of the treatment group mice. The index of livers was calculated as W_l/W_m, where W_l was the average livers weight (g) of each group and W_m was the average mouse body weight (g) of each group. The index of spleen was calculated as W_s/W_m, where W_s was the average spleen weight (mg) of each group and W_m was the average mouse body weights (g) of each group. Then samples of the tumors were fixed in 10% neutral buffered formalin, embedded in paraffin, sectioned at 4 mm, and processed according to the hematoxylin and eosin (HE) staining protocol. Quantitative analysis was made in a blinded manner under a light microscope. Each section was examined at magnification (×100). Computer-assisted image tracking was used to calculate the positive tumor areas. The results were regarded as the mean ± SD of eight different sections.

3.3. Immunohistochemical analysis of nuclear factor-κB (NF-κB), and cycloxygenase-2 (COX-2)

An immunohistochemical study was performed with monoclonal antibodies against NF-κB (P65) and COX-2. The final dilution for these antibodies was 1:50 and 1:150, respectively. With all antibodies, a three-step indirect immunohistochemical method was used. The paraffin section of the S180 tumor was dewaxed to water, incubated in 3% H_2O_2 for 10 min at room temperature, washed three times with 0.01 mol/L PBS, heat induced epitope retrieval. Then incubated with 5-10% normal goat serum for 10 min, pour to serum, not washed. Then incubated with primary antibodies for 1-2 h at 37 °C, washed three times with 0.01 mol/L PBS. The secondary antibodies biotin-labeled were diluted to 1:250 in PBS prior to use, incubated for 30 min at 37 °C, and washed three times with 0.01 mol/L PBS. Finally incubation with an appropriate amount of a horseradish peroxidase-labeled streptavidin peroxidase working solution for 30 min at 37 °C, and washed three times with 0.01 mol/L PBS. Coloration with DAB for 5 min, and washed by running water quietly. Sections were redyed with haematoxylin, every piece of the sections was dehydrated, made to be transparent in a conventional way, and then observed and photographed under a microscope. Primary antibodies were replaced by PBS for the negative controls. None of the controls revealed any specific signal.

3.4. Acute toxicity

Kunming mice of both sexes, weighing 18–22 g, were divided into two groups of 20 animals matched in weight and size. The mice were placed in cages and kept under standard environmental conditions with a standard rodent diet and water *ad libitum*

under a 12 h light-dark cycle. They were deprived of food for 24 h but allowed free access to tap water throughout the experiments. The maximum suspended dose (50 mg/mL) of T-OA was prepared in bean oil solution. Then one group of 20 mice of both sexes received the maximum tolerated dose (0.4 mL/10 g) by oral administration every four hours. The total administration of T-OA was 6 g/kg during 12 h. Similarly, the other 20 mice (control group) received bean oil (0.4 mL/10 g) via gavage for three times in 12 h. The general behavior of the mice was observed continuously for 1 h after the treatment and then intermittently for 4 h, and thereafter over a period of 24 h. The mice were further observed for up to 14 days following treatment for any signs of toxicity and deaths, and the latency of death. Behavior, toxic effects and mortality response were recorded.

3.5. Pharmacokinetic assay

3.5.1. Preparation of standard solution, quality control working solution, and samples

T-OA stock solutions (2.0500 mg/mL) and IS working solution (40.1600 μg/mL) were prepared with methanol. A series of T-OA standard working solutions at 2.0500, 4.1000, 8.2000, 16.4000, 20.5000, 41.0000, 51.2500 and 82.0000 μg/mL were serially diluted in methanol from the stock solution. Quality control (QC) working solutions (8.2500, 25.6250, and 65.6000 μg/mL) of T-OA were prepared in the same way. All the solutions were stored at 4 °C and brought to room temperature before using.

Healthy SD rats were fasted overnight and water was allowed *ad libitum* throughout the experiments. Blood was obtained from the ophthalmic vein and collected with dried heparinized tubes. The plasma was separated by centrifugation at 3,000 g for 10 min. Plasma stored in a freezer at −20 °C was thawed at 4 °C before treatment. The plasma samples were prepared according to the method described by Li et al. (2011), with minor modifications. Briefly, 5 μL IS working solution was added to the plasma samples (100 μL), followed by vortexing for 1 min. For extraction, 300 μL acetonitrile was added to the mixture under vortex-mixing for 5 min. The mixture was then centrifuged at 12,000g for 5 min in a refrigerated centrifuge at 4 °C. The organic phase was transferred into a clean test tube and was evaporated to dryness in a water bath at 40 °C under a gentle stream of nitrogen. The residue was reconstituted in methanol and was then vortex-mixed for 1 min. The solution was centrifuged at 12,000g for 5 min and a 10 μL supernatant was injected into the HPLC system for analysis.

3.5.2. Method validation

3.5.2.1. Calibration curve and linearity

The calibration curve for T-OA was prepared by spiking a series of 100 μL blank rat plasma with 10 μL standard working solutions. Then 5 μL IS working solution was added to these plasma samples, respectively. The calibration curve was constructed by linear least-squares regression analysis plotting of the plasma samples' peak area ratios of T-OA to the IS *versus* the corresponding working solution concentrations of T-OA. Thus, the linearity was evaluated by the linear correlation coefficient (r) of the calibration curve.

3.5.2.2. Precision, accuracy, limit of detection, and quantitation

The precision was expressed as the intra-day and inter-day relative standard deviation (RSD). Quality control samples (QC samples) of low, middle and high concentration were prepared by blank plasma spiked with QC working solutions of T-OA, respectively. The intra-day RSD was assessed by determining QC samples at the three concentration levels five times on the same day, whilst the inter-day RSD was determined by repeated analysis on six consecutive days. The accuracy (relative recovery) was calculated from the QC samples theoretical concentrations (C_{the}) and the mean QC samples (n = 5) observed concentration (C_{obs}) according to the formula: relative recovery (%) = (C_{obs}/C_{the}) × 100%. The limit of detection (LOD) was determined as the plasma concentration giving a signal-to-noise ratio of 3 and the limit of quantitation (LOQ) was the lowest concentration on the standard curve (Hou et al. 2012).

3.5.2.3. Extraction recovery and stability

The extraction recovery of T-OA from the QC samples contained relative recovery and absolute recovery, which were assayed and calculated by the following equation: relative recovery (%) = (C_{obs}/C_{the}) × 100%, which was also expressed as the accuracy (Li et al. 2011); absolute recovery (%) = [A_{obs}/A_{the}] × 100%, where A_{the} is the mean T-OA peak area (n = 5) generated by the QC samples, A_{obs} is the mean peak area (n = 5) obtained by 10-fold-methanol dilution of QC working solutions, which were the same concentration as QC samples.

The freeze–thaw stability of T-OA was evaluated by analyzing the QC samples after three freezing (−20 °C) and thawing (ambient) cycles. The short-term stability of T-OA in rat plasma was assessed by placing the QC samples at room temperature for 24 h before extraction and analysis. The concentration of T-OA assayed in the above samples after each treatment was compared with the initial value.

3.5.3. Pharmacokinetic study and data analysis

T-OA was suspended in bean oil solution before using. Before drug administration, six SD rats were fasted overnight but water was allowed *ad libitum*. A single dose (300 mg/kg) of T-OA solution was administered orally. The blood samples were collected in dried heparinized tubes at 1, 2, 4, 6, 8, 10, 12, 16, and 24 h after drug administration. The plasma samples were centrifuged, then frozen and stored at −20 °C until analysis.

The concentration–time profile and the main pharmacokinetic parameters were processed by the software of WinNonlin (Version 5.2, Pharsight Corp., Mountain View, California, USA) with the non-compartmental model.

3.6. Statistical analysis

All data are expressed as mean ± SD. Statistical comparisons between groups performed using 1-way ANOVA followed by Student's t-test and $P < 0.05$ was considered significant.

Acknowledgments: This study was financially supported by the National Natural Science Foundation of China (No. 81173519) and the Innovation Team Project Foundation of Beijing University of Chinese Medicine (Lead Compound Discovering and Developing Innovation Team Project Foundation, No. 2011-CXTD-15).

References

Aggarwal BB (2004) Nuclear factor-kappaB: the enemy within. Cancer Cell 6: 203–208.

Breinig M, Schirmacher P, Kern MA (2007) Cyclooxygenase-2 (COX-2)–a therapeutic target in liver cancer? Curr Pharm Des 13: 3305–3315.

Cathcart MC, O'Byrne KJ, Reynolds JV, O'Sullivan J, Pidgeon GP (2012) COX-derived prostanoid pathways in gastrointestinal cancer development and progression: novel targets for prevention and intervention. Biochim Biophys Acta 1825: 49–63.

Cesta MF (2006) Normal structure, function, and histology of the spleen. Toxicol Pathol 34: 455–465.

Chen Y, Chen JW, Xu SS, Wang Y, Li X, Cai BC, Fan NB (2012) Antitumor activity of annonaceous acetogenins in HepS and S180 xenografts bearing mice. Bioorg Med Chem Lett 22: 2717–2719.

Chiou WL, Riegelman S (1971) Pharmaceutical applications of solid dispersion systems. J Pharm Sci 60: 1281–1302.

Hao YZ, Wang PL, Hong Y, Lei HM (2010) Synthesis and structure identification of tetramethylpyrazine-protocatechuic acid and effects on hypoxic-ischemic brain damage. Pharmacol Clin Chin Materia Med 26: 41–45.

He X, Pei L, Tong HH, Zheng Y (2011) Comparison of spray freeze drying and the solvent evaporation method for preparing solid dispersions of baicalein with Pluronic F68 to improve dissolution and oral bioavailability. AAPS PharmSci Tech 12: 104–113.

Hou SY, Wang F, Li YM, Li Y, Wang MQ, Sun DJ, Sun CH (2012) Pharmacokinetic study of mangiferin in human plasma after oral administration. Biopharm Drug Dispos 132: 289–294.

Jeong DW, Kim YH, Kim HH, Ji HY, Yoo SD, Choi WR, Lee SM, Han CK, Lee HS (2007) Dose-linear pharmacokinetics of oleanolic acid after intravenous and oral administration in rats. Biopharm Drug Dispos 28: 51–57.

Jiang Y, Jiang X, Law K, Chen Y, Gu J, Zhang W, Xin H, Sha X, Fang X (2011) Enhanced anti-tumor effect of 9-nitro-camptothecin complexed by hydroxypropyl-β-cyclodextrin and safety evaluation. Int J Pharm 415: 252–258.

Kang CH, Choi YH, Choi II-W, Lee JD, Kim GY (2011) Inhibition of lipopolysaccharide-induced iNOS, COX-2, and TNF-α expression by aqueous extract of *Orixa japonica* in RAW 264.7 Cells via Suppression of NFκB Activity. Trop J Pharm Res 10: 161–168.

Lee JI, Burckart GJ (1998) Nuclear factor kappa B: important transcription factor and therapeutic target. J Clin Pharmacol 31: 981–993.

Lee YB, Gong YD, Kim DJ, Ahn CH, Kong JY, Kang NS (2012) Synthesis, anticancer activity and pharmacokinetic analysis of 1-[(substituted 2-alkoxyquinoxalin-3-yl)aminocarbonyl]- 4-(hetero)arylpiperazine derivatives. Bioorg Med Chem 20: 1303–1309.

Leuner C, Dressman J (2000) Improving drug solubility for oral delivery using solid dispersions. Eur J Pharm Biopharm 50: 47–60.

Li S, Chen H, Wang X, Wu J, Jiang J, Wang Y (2011) Pharmacokinetic study of a novel stroke therapeutic, 2-[[(1,1-dimethylethyl)oxidoimino]methyl]-3,5,6-trimethylpyrazine, by a simple HPLC-UV method in rats. Eur J Drug Metab Pharmacokinet 36: 95–101.

Li XY, He JL, Liu HT, Li WM, Yu C (2009) Tetramethylpyrazine suppresses interleukin-8 expression in LPS-stimulated human umbilical vein endothelial cell by blocking ERK, p38 and nulear factor-kappaB signaling pathways. J Ethnopharmacol 125: 83–89.

Liao N, Ao MZ, Zhang P, Yu LJ (2012) Extracts of Lycoris aurea induce apoptosis in murine sarcoma S180 cells. Molecules 17: 3723–3735.

Liu L, Wang X (2007) Improved dissolution of oleanolic acid with ternary solid dispersions. AAPS PharmSci Tech 8: 267–271.

Mammon K, Savion S, Keshet R, Aroch I, Orenstein H, Fein A, Torchinsky A, Toder V (2006) Expression of apoptosis-associated molecules in the fetoplacental unit of cyclophosphamide- treated mice. Reprod Toxicol 22: 774–782.

Mazhar D, Gillmore R, Waxman J (2005) COX and cancer. QJM 98: 711–718.

Nagendraprabhu P, Sudhandiran G (2011) Astaxanthin inhibits tumor invasion by decreasing extracellular matrix production and induces apoptosis in experimental rat colon carcinogenesis by modulating the expressions of ERK-2, NFkB and COX-2. Invest New Drugs 29: 207–224.

Ni M, Chen ZS, Peng YH (2005) Clinical study of intraperitoneal chemotherapy plus Shiquandabu drink on advanced gastric cancer. Chin Clin Oncol 10: 288–290.

Olivera A, Moore TW, Hu F, Brown AP, Sun A, Liotta DC, Snyder JP, Yoon Y, Shim H, Marcus AI, Miller AH, Pace TW (2012) Inhibition of the NF-κB signaling pathway by the curcumin analog, 3,5-Bis(2-pyridinylmethylidene)-4-piperidone (EF31): anti-inflammatory and anti-cancer properties. Int Immunopharmacol 12: 368–377.

Orlowski RZ, Baldwin AS Jr (2002) NF-kappaB as a therapeutic target in cancer. Trends Mol Med 8: 385–389.

Plummer SM, Holloway KA, Manson MM, Munks RJ, Kaptein A, Farrow S, Howells L (1999) Inhibition of cyclo-oxygenase 2 expression in colon cells by the chemopreventive agent curcumin involves inhibition of NF-kappaB activation via the NIK/IKK signalling complex. Oncogene 18: 6013–6020.

Qiu F, Zhou S, Fu S, Kong W, Yang S, Yang M (2012) LC-ESI-MS/MS analysis and pharmacokinetics of 6'-hydroxy justicidin A, a potential antitumor active component isolated from Justicia procumbens, in rats. J Pharm Biomed Anal 70: 539–543.

Santhi WS, Sebastian P, Varghese BT, Prakash O, Pillai MR (2006) NF-kappaB and COX-2 during oral tumorigenesis and in assessment of minimal residual disease in surgical margins. Exp Mol Pathol 81: 123–130.

Sarkar FH, Adsule S, Li Y, Padhye S (2007) Back to the future: COX-2 inhibitors for chemoprevention and cancer therapy. Mini Rev Med Chem 7: 599–608.

Sinha S, Ali M, Baboota S, Ahuja A, Kumar A, Ali J (2010) Solid dispersion as an approach for bioavailability enhancement of poorly water-soluble drug ritonavir. AAPS PharmSci Tech 11: 518–527.

Sivaramakrishnan V, Niranjali Devaraj S (2009) Morin regulates the expression of NF-kappaB-p65, COX-2 and matrix metalloproteinases in diethylnitrosamine induced rat hepatocellular carcinoma. Chem Biol Interact 180: 353–359.

Suh SJ, Jin UH, Kim KW, Son JK, Lee SH, Son KH, Chang HW, Lee YC, Kim CH (2007) Triterpenoid saponin, oleanolic acid 3-O-beta-d-glucopyranosyl(1–>3)-alpha-l- rhamnopyranosyl(1–>2)-alpha-l-arabinopyranoside (OA) from Aralia elata inhibits LPS-induced nitric oxide production by down-regulated NF-kappaB in raw 264.7 cells. Arch Biochem Biophys 467: 227–233.

Suzuki S, Singhirunnusorn P, Nakano H, Doi T, Saiki I, Sakurai H (2006) Identification of TNF-alpha-responsive NF-kappaB p65-binding element in the distal promoter of the mouse serine protease inhibitor SerpinE2. FEBS Lett 580: 3257–3262.

Tang TC, Poon RT, Lau CP, Xie D, Fan ST (2005) Tumor cyclooxygenase-2 levels correlate with tumor invasiveness in human hepatocellular carcinoma. World J Gastroenterol 11: 1896–1902.

Wang PL, Cheng YT, Xu K, An YW, Wang W, Li QS, Han QJ, Li Q, Zhang HG, Lei HM (2013) Synthesis and anti-tumor evaluation of one novel tetramethylpyrazine-rhein derivative. Asian J Chem 25: In press.

Wang PL, She GM, Yang YN, Li Q, Zhang HG, Liu J. Cao YQ, Xu X, Lei HM (2012) Synthesis and biological evaluation of new ligustrazine derivatives as anti-tumor agents. Molecules 17: 4972–4985.

Wu DD, Gao YF, Chen LX, Qi YM, Kang QZ, Wang HL, Zhu LY, Ye Y, Zhai MX (2010) Anti-tumor effects of a novel chimeric peptide on S180 and H22 xenografts bearing nude mice. Peptides 31: 850–864.

Xiao YY, Ping QN, Chen ZP (2007) The enhancing effect of synthetical borneol on the absorption of tetramethylpyrazine phosphate in mouse. Int J Pharm 337: 74–79.

Xu QM, Shu Z, He WJ, Chen LY, Yang SL, Yang G, Liu YL, Li XR (2012) Antitumor activity of Pulsatilla chinensis (Bunge) Regel saponins in human liver tumor 7402 cells in vitro and in vivo. Phytomedicine 19: 293–300.

Yin J, Yu C, Yang Z, He JL, Chen WJ, Liu HZ, Li WM, Liu HT, Wang YX (2011) Tetramethylpyrazine inhibits migration of SKOV3 human ovarian carcinoma cells and decreases the expression of interleukin-8 via the ERK1/2, p38 and AP-1 signaling pathways. Oncol Rep 26: 671–679.

Yoon JM, Lim JJ, Yoo CG, Lee CT, Bang YJ, Han SK, Shim YS, Kim YW (2005) Adenovirus-uteroglobin suppresses COX-2 expression via inhibition of NF-kappaB activity in lung cancer cells. Lung Cancer 48: 201–209.

Zhang JL, Wang H, Chen C, Pi HF, Raun HL, Zhang P, Wu JZ (2009) Addictive evaluation of cholic acid-verticinone ester, a potential cough therapeutic agent with agonist action of opioid receptor. Acta Pharmacol Sin 30: 559–566.

Zhang JL, Wang H, Pi HF, Ruan HL, Zhang P, Wu JZ (2009) Structural analysis and antitussive evaluation of five novel esters of verticinone and bile acids. Steroids 74: 424–434.

Zhang PX, Li HM, Chen D, Ni JH, Kang YM, Wang SQ (2007) Oleanolic acid induces apoptosis in human leukemia cells through caspase activation and poly (ADP-ribose) polymerase cleavage. Acta Bioch Bioph Sin 39: 803–809.

Zhong B, Cai X, Chennamaneni S, Yi X, Liu L, Pink JJ, Dowlati A, Xu Y, Zhou A, Su B (2012) From COX-2 inhibitor nimesulide to potent anticancer agent: synthesis, in *vitro*, in *vivo* and pharmacokinetic evaluation. Eur J Med Chem 47: 432–444.